Determination of arsenic in water using fluorescent ZnO quantum dots

Journal:	*Analytical Methods*
Manuscript ID	AY-ART-09-2015-002472.R1
Article Type:	Paper
Date Submitted by the Author:	26-Nov-2015
Complete List of Authors:	Pal, Sudip; Assam University, Department of Chemistry Akhtar, Nargis; Assam University, Department of Chemistry Ghosh, Sujit; Assam University, Department of Chemistry

Analytical Methods

Dynamic Article Links►

Cite this: DOI: 10.1039/c0xx00000x

www.rsc.org/xxxxxx

Paper

Determination of arsenic in water using fluorescent ZnO quantum dots

Sudip Kumar Pal, Nargis Akhtar and Sujit Kumar Ghosh*

Received (in XXX, XXX) XthXXXXXXXXX 20XX, Accepted Xth XXXXXXXXX 20XX
DOI: 10.1039/b000000x

Stabiliser-free zinc oxide (ZnO) quantum dots (QDs) have been synthesised by refluxing zinc acetate dihydrate in methanol under alkaline condition and were re-dispersed into water by centrifugation. The ultrasmall particles so obtained have been characterised by absorption and fluorescence spectroscopy, transmission electron microscopy and selected area electron diffraction studies. The as-prepared fluorescent ZnO QDs have been employed as greener indicator for selective and ultrasensitive detection of highly toxic arsenic in aqueous solution. Since fluorescence spectroscopy is a very sensitive technique, fluorescence quenching behaviour of ZnO QDs upon addition of arsenic compounds has been utilised as a sensing platform for the quantification of arsenic in parts-per-billion (ppb) level. The interaction of the arsenic species with the ZnO QDs has been elucidated by Fourier transform infrared spectroscopy, zeta potential measurements and dynamic light scattering studies. Three different calibration curves for arsenic(III), arsenic(V) and total arsenic [arsenic(III) + arsenic(V)] have been set up in the dynamic range of 10-100 ppb and the corresponding limit of detection is 27, 7 and 28 ppb respectively. The method is free from common interferences and applicable for real sample analysis.

1. Introduction

Elemental arsenic and its compounds are highly toxic substances and widely distributed in the earth crust.[1] Depending on the environmental condition, arsenic can exist in two different oxidation states, As(III) and As(V) in natural water and its direct exposure is detrimental to humans, animals and the entire ecosystem.[2] Exposure to arsenic above a particular concentration can cause a variety of adverse health effects, including, dermal changes and respiratory, cardiovascular, gastrointestinal, genotoxic, mutagenic, and carcinogenic effects and the collective term of the diseases caused by chronic exposure to arsenic is called ‘arsenicosis’.[3] Arsenic poisoning is the second most important health hazard related to drinking water after contamination by pathogenic microorganism.[4] Contamination of drinking water by arsenic is found in many parts of the world, such as, Bangladesh, India, Nepal, China, Taiwan, Vietnam, Inner Mongolia, New Zealand, Philippines, Hungary, Cambodia, Ghana, Chile, Mexico, Argentina and the United States.[5] Therefore, detection and determination of arsenic and its compounds, especially, when present at relatively low concentrations, is crucial in ecological and environmental sciences. According to the World Health Organization (WHO) and the U. S. Environmental Protection Agency (EPA), the primary maximum contaminant level (MCL) for the arsenic in the drinking water is 10 ppb.[6,7] It is known that ZnO is a IIb–VI compound semiconductor with a direct wide band gap of 3.37 eV and a large exciton binding energy of 60 meV at room temperature which has been demonstrated to exhibit enormous applications in miniaturizing electronic and optoelectronic devices.[8] In addition to these physicochemical properties, numerous environmental advantages, such as, non-toxicity, corrosion resistance, recyclability and easy disposal of the material have encouraged its application as greener materials for environmental engineering and processes monitoring.[9] It is, now, well established in the literature that ZnO at the nanoscale dimension may have superior optical properties over bulk material due to the quantum confinement effect.[10] The high optical transparency and luminescent properties in the near ultraviolet and the visible regions along with its excellent biocompatibility have enable their applications in a diverse range of niche applications.[11]

Numerous analytical techniques have been employed for the determination of arsenic, which include, inductively coupled plasma mass spectrometry (ICP-MS),[12] graphite furnace atomic absorption spectrometry (GFAAS)[13] and high performance liquid chromatography (HPLC) with ICP-MS[14] etc. Although, AAS or HPLC methods are very sensitive and effective, sophisticated instrumentation and exquisite expertise are pre-requisites for the determination of arsenic with these techniques. As alternative to these conventional methodologies, nanotechnology is being exploited for the quantification of arsenic in natural water and several other samples using seminal electrochemical and spectroscopic techniques. Pal and co-workers[15] described a method for arsenic determination using the reduction of methylene blue by arsine in sodium dodecyl sulfate micellar medium which was, further, facilitated in the presence of Ag or Au nanoparticles. Compton and colleagues[16] reported anodic stripping voltammetry for the detection of As(III) using gold nanoparticle-modified glassy carbon electrodes. Loung and colleagues[17] designed a flow analysis technique by the electrochemical deposition of gold nanoparticles on a dual glassy carbon electrode for the determination of arsenite in aqueous solution. Yang and colleagues[18] employed surface enhanced Raman spectroscopic technique using Langmuir–Blodgett assemblies of polyhedral Ag nanocrystals as highly active SERS substrates that can perform low-level arsenate and arsenite sensing in contaminated water. Zhou and co-authors[19] have synthesised varieties of nanoparticle-assembly *via* controlling the concentration of arsenic-binding aptamers in crystal violet solution for As(III) detection in aqueous solution based on a resonance Rayleigh scattering spectral assay. Yuan and colleagues[20] have performed square wave anodic stripping

---

Department of Chemistry, Assam University, Silchar-788011, India
E-mail: sujit.kumar.ghosh@aus.ac.in

voltammetry for the determination of arsenic(III) by dropping Fe_3O_4 nanoparticles onto glassy carbon electrode and subsequent electrodeposition of gold nanoparticles. Bermejo-Barrera and co-authors[21] have exploited the surface plasmon absorption of gold nanoparticles for the detection of arsenic at low concentration. Liu and Liu[22] have employed fluorescently-labeled DNA oligonucleotides *via* the backbone phosphate adsorbed onto iron oxide nanoparticles and fluorescence enhancement upon addition of arsenate by replacement DNA oligonucleotides rendered the detection of the analyte down to 300 nM.

In this article, we have exploited the photoluminescence properties of water-soluble ZnO QDs for the greener determination of arsenic in aquatic environment. The ultrasmall ZnO particles have been characterised by absorption and fluorescence spectroscopy, transmission electron microscopy (TEM), high resolution transmission electron microscopy (HRTEM), selected area electron diffraction (SAED) pattern analysis. The mechanism of binding of the arsenic species to the ZnO particles has been substantiated by Fourier transform infrared (FTIR) spectroscopy, zeta potential measurements and dynamic light scattering (DLS) studies. It is seen that fluorescence of the quantum dots become quenched in the presence of arsenic analytes and is extremely sensitive to the arsenic concentration in parts-per-billion (ppb) level in water samples. Therefore, fluorescence quenching behaviour of as-synthesised ZnO QDs could be manipulated to engineer selective and ultrasensitive detection of highly toxic arsenic in water, at parts-per-billion concentrations.

2. Experimental

2.1. Reagents and instruments

All the reagents used were of analytical reagent grade. Zinc acetate dihydrate ($Zn(OOCCH_3)_2.2H_2O$), sodium (meta)arsenite ($NaAsO_2$), disodium hydrogen arsenate heptahydrate ($Na_2HAsO_4.7H_2O$), ethylenediamminetetraacetic acid disodium salt dihydrate ($C_{10}H_{14}N_2Na_2O_8.2H_2O$), sodium dihydrogen phosphate ($NaH_2PO_4.H_2O$) and sodium hydrogen phosphate (Na_2HPO_4) were purchased from Sigma-Aldrich and were used without further purification. Potassium hydroxide (S. D. Fine Chemicals, India), and methanol (Sisco Research Laboratories Pvt. Ltd., India) were used as received. Sodium phosphate buffer solution of pH~7.0 was prepared by taking 0.5836 g of $NaH_2PO_4.H_2O$ and 0.8195 g of anhydrous Na_2HPO_4 and volume was made to 1 L with distilled water. Double distilled water was used throughout the course of the investigation. The temperature was 298±1 K for all experiments.

Absorption spectra were recorded in a PerkinElmer UV-VIS-NIR digital spectrophotometer taking the sample in 1 cm well-stoppered quartz cuvette. Fluorescence spectra were recorded with a PerkinElmer LS-45 spectrofluorimeter equipped with a pulsed xenon lamp and a photomultiplier tube with R-928 spectral response. The spectrofluorimeter was linked to a personal computer and utilised the FL WinLab software package for data collection and processing. Transmission electron microscopy (TEM) and selected area electron diffraction (SAED) pattern was carried out on a JEOL JEM 2100 microscope with a magnification of 200 kV. Samples were prepared by placing a drop of solution on a carbon coated copper grid. Atomic absorption spectroscopy (AAS) was performed on a Varian Spectr AA110 atomic absorption spectrometer. Dynamic light scattering (DLS) study was performed using a NanoZS (Malvern) instrument after filtering the sample solution with Milipore syringe filter (0.2 μm pore size). Finally, the zeta potential of the ZnO QDs before and after addition of arsenic solution was measured by Nano-ZS (Malvern) test measurement system. For all optical as well as mobility measurements, nanoparticles were isolated from their methanolic dispersion and finally, redispersed in water.

2.2. Synthesis of zinc oxide quantum dots

Stabiliser-free ZnO QDs were synthesised by the precipitation of Zn^{2+} with ^{-}OH in an alcoholic solution by following the procedure of Weller group.[23] An amount of 0.055 g zinc acetate dihydrate [$Zn(ac)_2.2H_2O$] was dissolved in 25 mL of methanol in a double-necked round-bottom flask by refluxing the mixture in a water bath at 45 ^{0}C. After 45 min, the temperature of the reaction mixture was increased to 60 ^{0}C. After 15 min, 13.5 mL KOH solution (0.1 mM) was added to the mixture instantaneously and curdy white colouration was obtained indicating the formation of ZnO particles. The refluxing was continued for another 1 h and the colour of the solution became white indicating the completion of the reaction. Then, the heat was removed from the reaction mixture and was stirred for 12 h at room temperature. The dispersion so obtained was washed for 3–4 times with methanol and separated by centrifugation at 10,000 rpm for 1 min. The particles were, finally, redispersed in water with the help of ultrasonic treatment and stored in the dark. The dispersion was found to be stable for a couple of months without any sign of agglomeration or precipitation of the particles. The particles obtained by this method could, even, be stored as a powder and redispersed in water as and whenever required.

2.3. Determination of arsenic with zinc oxide quantum dots

Three different batches of ten sets of solutions of arsenic compounds (10-100 ppb) have been prepared in sodium phosphate buffer solution in the test tubes. Then, a particular concentration (1.0 μM) of ZnO QDs was added in each set of solutions. The total volume of the solutions was maintained to 3.0 mL and the pH of all the solutions was adjusted ~7.0. All the solutions were allowed to incubate for 1 h and the fluorescence spectrum of each solution was measured in the spectrofluorimeter.

3. Results and discussion

Recently, quantum dots have drawn extensive research interest due to their unique optical properties that arises from

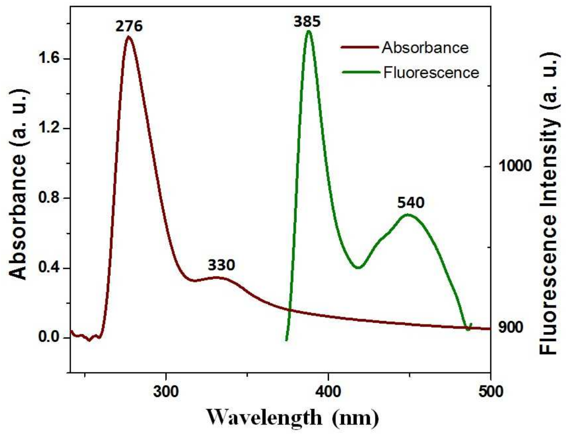

Fig. 1. Absorption (1.0 mM) and fluorescence (1.0 μM) spectra of free ZnO quantum dots.

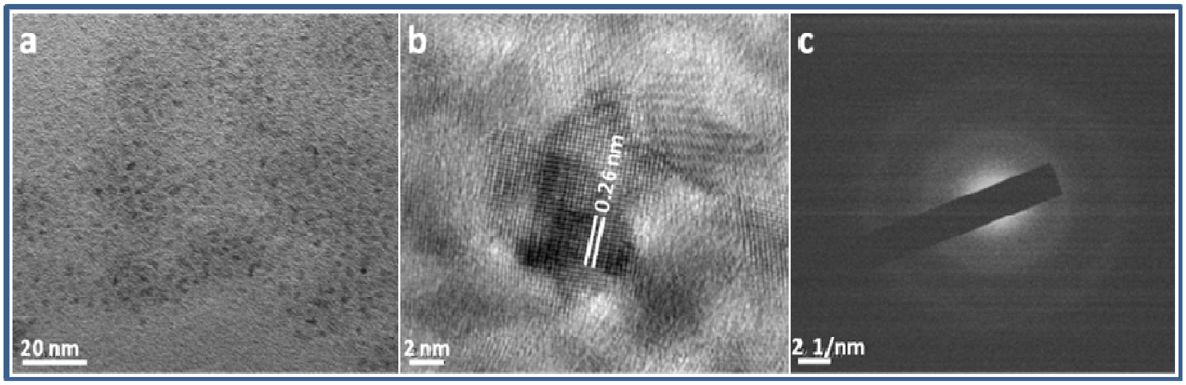

Fig. 2. (a) Transmission electron micrograph, (b) high resolution transmission electron micrograph and (c) selected area electron diffraction pattern of the ZnO particles

their small size and quantum confinement effect.[24] From the text book chemistry, it is known that Zn^{2+} conforms to tetrahedral geometry with zero crystal field stabilization energy due to the 3d^{10} electronic configuration.[25] Therefore, it shows very good electronic transitions from valance band to conduction band and could act as a very good sensor. Fig. 1 shows the room temperature optical absorption and emission spectra of free ZnO quantum dots. It is seen that free ZnO exhibit two absorption peaks, one is at wavelength 276 nm (4.49 eV) and another at 330 nm (3.76 eV) which are the characteristics of spherical ZnO nanoparticles. In case of semiconductor nanoparticles, the Fermi energy level lies in-between the valance and conduction band, which comprises of discrete energy states due to strong electron confinement. These two peaks arise due to the excitonic transitions between the trapped energy states situated in between the confinement region.[25] The optical band edge bears the characteristic electronic transition energy taken place to promote the electrons to the energy states in conduction band from the valence band, including, excitonic effects.[26] The fluorescence spectrum (λ_{ex} ~ 276 nm) of the ZnO particles at the nanoscale dimension exhibits a narrow near-band-edge UV emission with maximum at 385 nm (3.22 eV) and a weak broad green band with maximum at 540 nm (2.3 eV). The ultraviolet emission peak corresponds to an excitonic emission that could be attributed to the radiative recombination of a hole in the valence band and an electron in the conduction band;[27] whereas, the broad green emission band, known as a deep-level emission, is believed to be due to an electronic transition from a level close to the conduction band edge to a defect associated trap state, such as, oxygen vacancies, zinc vacancies, as well as donor–acceptor pairs.[28]

Transmission electron micrograph, high resolution transmission electron micrograph and selected area electron diffraction pattern of the ZnO particles are shown Fig. 2. From the TEM image (panel a), it is seen that the particles are spherical or nearly spherical and the particle size lies in the size range of 3 ± 0.5 nm. The HRTEM image (panel b) of single ZnO QDs exhibit a lattice fringe of 0.26 nm consistent with the d$_{002}$ spacing of wurtzite ZnO nanostructures.[29] From the SAED pattern (panel c), the diffraction rings which are consistent with reflections (100), (002), (101), (102), (110) correspond to the hexagonal wurtzite phase of ZnO nanoparticles.[30]

The changes in the absorption spectrum of ZnO QDs were followed upon addition of arsenic analytes. However, as the concentration of the arsenic species is in the ppb level, insignificant damping was seen in the absorption spectrum of ZnO QDs. Therefore, since ZnO QDs are fluorescent, the sensitivity of the emission behaviour of the ultrasmall particles has been exploited for the determination of arsenic in aqueous solution. The concentration of ZnO (1.0 μM) was kept constant in all sets of solutions and the fluorescence spectrum of each solution (λ_{ex} ~ 276 nm) was measured with the variation of concentrations of arsenic analytes in the solutions. We have, judiciously, studied the effects of such changes on the near-band-edge UV emission that is relatively dominant over the weak broad green band in the fluorescence spectrum of ZnO QDs. Fig. 3 shows the fluorescence spectra of ZnO QDs (1.0 μM) in the presence of different concentrations (10 - 100 ppb) of As(III), As(V) and same concentration of individual As(III) and As(V) but total concentration of arsenic being different in different sets. It is to be mentioned that the intensity (I_0) of ZnO QDs in the absence of any quencher is 998 a. u. It is seen that ZnO QDs suffers quenching of their fluorescence upon addition of arsenic analytes irrespective of the oxidation

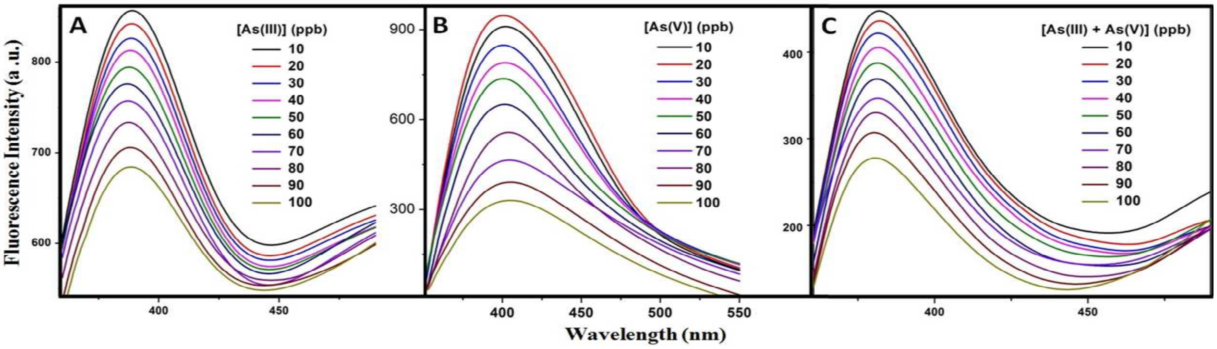

Fig. 3. Fluorescence spectra of ZnO quantum dots (1.0 μM) in the presence of (A) different concentrations (10 - 100 ppb) of As(III); (B) different concentrations (10 - 100 ppb) of As(V) and (C) mixture of equal concentration of As(III) and As(V) but total concentration of arsenic being different (10 - 100 ppb) in different sets. The pH of all the solutions was adjusted ~7.0 with sodium phosphate buffer solution.

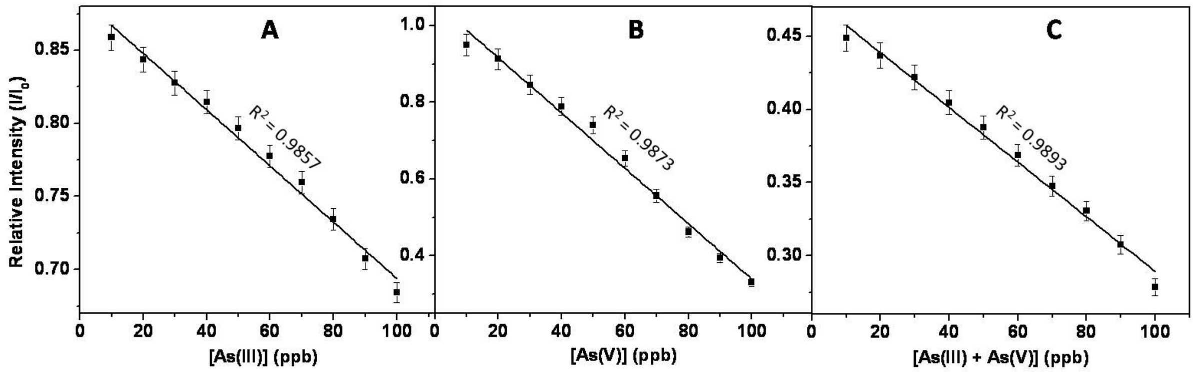

Fig. 4. Linear regression analysis showing relative fluorescence efficiency as a function of (A) different concentration As(III); (B) different concentrations of As(V) and (C) different total concentration of [As(III) + As(V)] bearing equal concentration of As(III) and As(V) in the mixture.

states.[31] The salient feature of analytical importance is that the intensity of UV emission is, gradually, quenched with increase in concentration of the arsenic analytes in solution while the emission maximum becomes slightly blue shifted. Upon careful observation, it is conceived that the blue shift for both As(III) and As(V) are not pronounced, whilst the shift for the combination of these two ions are much more clear. The UV band near 385 nm arises from an exciton decay as it is close to the position of the band edge and moves to shorter wavelengths as the incorporated arsenic species in ZnO are deep acceptor because of their large ionic radii as compared to O.[32] Addition of the two different oxidation states of arsenic in the solution, provides excess vibrational levels that corresponds to the unattainable band gap due to the presence of As(III) and As(V) alone; therefore, the ZnO QDs could access the highest possible energetic configuration through the excess available vibrational staircase and moves to shorter wavelengths.[32] However, based on the linear dose response of arsenic analytes on the emission properties of ZnO QDs, three different calibration curves have been set up for three different categories of arsenic analytes as shown in Fig. 4. It is observed that this simple dependence allows for arsenic quantification in the dynamic range of 10–100 ppb of arsenic analytes in aqueous solution. Moreover, it is analysed that calibration curves for two most common oxidation states of arsenic are comparable which indicates that arsenic in both oxidation states impose nearly similar attributes to the emission characteristics of ZnO QDs. To further authenticate the fact, a series of mixtures of arsenic analytes were prepared where the concentration of individual As(III) and As(V) were same but the total concentration for all mixtures was different. Analytical results for the quantitative determination of three different categories of arsenic analytes are summarised in Table 1.

In the next step, the effect of common interferences has been examined for the fluorimetric determination of arsenic analytes in an aquatic environment. Therefore, we have also carried out studies with various common metal ions, such as, Ca(II), Fe(III), Mg(II), Ba(II), Mn(II), Pb(II), Cu(II) and Na(I) and anions, such as, Cl^-, Br^-, NO_3^-, PO_4^{3-} and CO_3^{2-} under similar experimental conditions that have been used for the determination of arsenic in the dispersion of ZnO QDs (1.0 μM). To study the influence of metal ions, metal salts, *viz.*, $CaCl_2$, $FeCl_3$, $MgCl_2$, $BaCl_2$, $MnCl_2$ $Pb(NO_3)_2$, $CuCl_2$ and NaCl and for anions, metal salts, *viz.*, NaCl, NaBr, $NaNO_3$, Na_3PO_4 and Na_2CO_3 were employed. The concentration of metal salts was maintained at 100 ppb and the pH of all the solutions was adjusted to ~7.0 with sodium phosphate buffer solution. Due to the adsorption of acetate counter ions, the surface of ZnO particles is negatively charged; therefore, anions could not interfere in the determination of arsenic species. The relative quenching efficiency, $((I_0\text{-}I/I_0)$ where, I_0 and I are the intensities of the ZnO QDs in the absence and presence of arsenic species) towards other metal ions is presented in Fig. 5. It is observed that, in the presence of other metal ions**,** quenching effect like that of the arsenic was not observed. However, since the contribution of sodium ions is ≤ 5% compared to that of arsenic, the contribution of sodium ions towards the fluorescence of ZnO QDs was neglected. These results suggest that naked fluorescent ZnO QDs are selective towards the detection of arsenic analytes in water samples. In

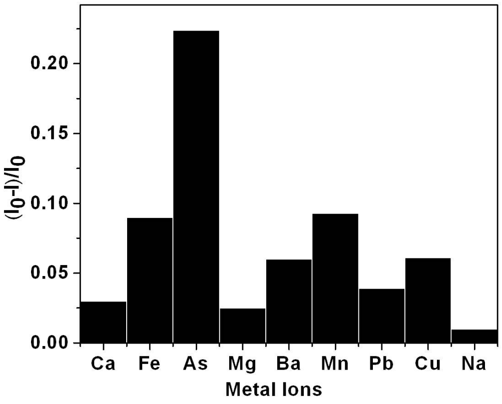

Fig. 5. Fluorescence quenching effect of ZnO in the presence of different metal ions under similar experimental conditions that have been used for the detection of arsenic in the dispersion of ZnO QDs (1.0 μM). The concentration of metal ions was maintained at 100 ppb. The pH of all the solutions was adjusted ~7.0 with sodium phosphate buffer solution.

Table 1. Statistical parameters for the determination of arsenic in water samples

Nature of arsenic	Slope	R^2	Standard deviation	[#]Limit of detection (LOD) (ppb)
As(III)	-0.0019	0.9857	0.0175	27.0
As(V)	-0.0072	0.9873	0.0175	7.0
As(III) + As (V)	-0.0019	0.9893	0.0175	28.0

[#]All LODs were calculated as LOD = 3 σ/m (where, σ is the standard deviation of the blank and m the slope of the calibration curve) metal oxide nanocrystals, the surface anions and cations have fewer numbers of nearest neighbours than the corresponding ions in the bulk.[33] Therefore, these surface anions and cations are co-ordinatively unsaturated that enable the ions to be active in bonding with adsorbates.[34] The fluorescence quenching of ZnO QDs is based on the adsorption of different metal ions on the surface of the ultrasmall particles. The incorporated donor atom of oxygen, presented in ZnO QDs, strongly govern the selective adsorption of different metal ions towards the particles. Moreover, acetate counter ions on the surface of ZnO QDs (synthesized using zinc acetate precursor) could adsorb the metal ions by an oxo-coordination mechanism. Therefore, the mechanism of adsorption may be electrostatic attraction or chelating mechanism between ZnO QDs and the metal ions. Thus, the difference in selectivity co-efficient of different metal ions towards the ZnO QDs leads to the selective interaction of different metal ions with the ultrasmall particles.[35]

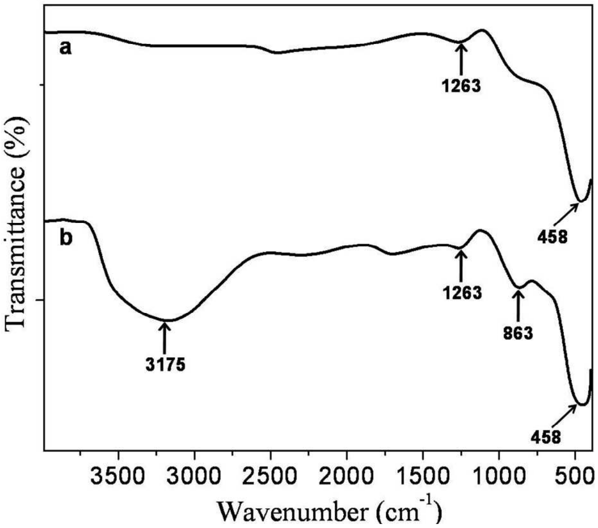

Fig. 6. Fourier transform infrared spectra of ZnO QDs in the (a) absence and (b) presence of As(III) species

Now, we have tried to elucidate the physical mechanism of interaction of arsenic species with the ZnO QDs. It is found that the near-band-edge UV emission is gradually quenched with increase in concentration of arsenic analytes. It is plausible that the positively charged arsenic sites of the arsenite/arsenate species become adsorbed onto the surface of naked ZnO QDs and attract electrons from the ultrasmall particles. Assuming that the UV emission arises due to the radiative recombination of a hole in the valence band and an electron in the conduction band, the attraction of electrons due to presence of large amount of arsenic species paves an avenue for the easy relaxation of the electrons from the exited state to the ground state leading to fluorescence quenching with consequent blue shifting of the emission maximum.[36] This hypothesis has been validated by Fourier transform infrared spectra, zeta potential and dynamic light scattering measurements. A better understanding of this analyte binding event on the surface of the QDs could be enunciated through Fourier transform infrared spectroscopy (Fig. 6). Before addition of arsenic (trace a), the main absorption band arising at *ca.* 458 cm^{-1}, could be assigned to stretching vibration of Zn–O bonds; the other absorption band at 1263 cm^{-1} corresponds to C–O stretching frequency due to adsorbed acetate counter ions.[37] After addition of arsenic species to the ZnO QDs (trace b), two new absorption bands arise, one is at 863 cm^{-1} which is due to the symmetry stretching vibration of As–O[38,39] and another strong absorption band at 3175 cm^{-1} that appears due to O–H stretching frequency from the adsorbed water from arsenic solution.[40] In the present experiment, free ZnO QDs possess the zeta potential of –38.7 mV while upon addition of a particular concentration of As(III) species (100 ppb), the zeta potential of the particles changes to –22.5 mV. This is due to the fact that, upon addition of arsenic analytes, As(III) sites become adsorbed onto the surface of negatively charged ZnO QDs (due to adsorption of negatively charged acetate counter ions)[41] and neutralises the surface charge from the ZnO QDs.[42] Dynamic light scattering measurements (Fig. 7) reveal that the number distribution hydrodynamic diameter[43] of free ZnO QDs (panel a) is *ca.* 122.4 ± 18.8 nm and upon addition of arsenic(III) analytes (100 ppb) (panel b), abruptly increases to *ca.* 396.1 ± 24.9 nm indicating the binding of the arsenic(III) species onto the particle surface. It is noted that there is a large discrepancy in the particle size obtained from TEM and DLS measurements and could be attributed to factors associated with the high vacuum conditions of TEM and the hydrodynamic and electrokinetic effects operative in DLS measurements. In the present experiment, negatively charged acetate counter ions become adsorbed onto the surface of ZnO QDs; thus, the average hydrodynamic particle diameter becomes different t o that of obtained under high vacuum conditions.[44] There is also a possibility of 'cation exchange reaction' upon addition of arsenic to the ZnO QDs. However, the appearance of any

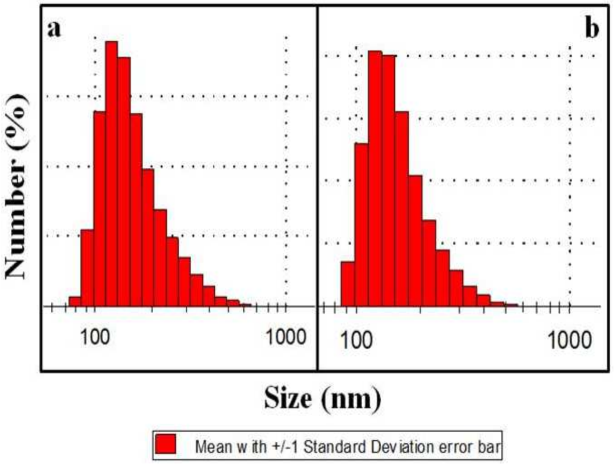

Fig. 7. Dynamic light scattering study of ZnO QDs (1.0 µM) in the (a) absence and (b) presence of As(III) species (100 ppb)

Table 2. Applicability of the present method for the determination of arsenic in real groundwater samples

Samples	#Concentration of arsenic (ppb)	
	Atomic absorption spectrophotometry	Present method§
Sample 1	90.2	90.5
Sample 2	80.5	80.5
Sample 3	70.5	70.9

\# Samples were collected from three different places of Barak Valley, Assam, India.

§An average of three determinations

characteristic absorption spectral features of arsenic species was not seen upon addition of arsenic to the ZnO QDs that rules out the possibility of any 'cation exchange reaction'.[45] Based on these results, it is convinced that arsenic analytes become adsorbed onto the ZnO QDs and consequently, quench the fluorescence of the ultrasmall particles. Since the quenching of fluorescence of ZnO QDs is based on the adsorption (not absorption) of the metal ions, the process is limited to the surface and would not penetrate into the bulk interior.[35] A schematic presentation showing the fluorescence quenching of ZnO QDs in the presence of arsenic analytes is shown in Scheme 1.

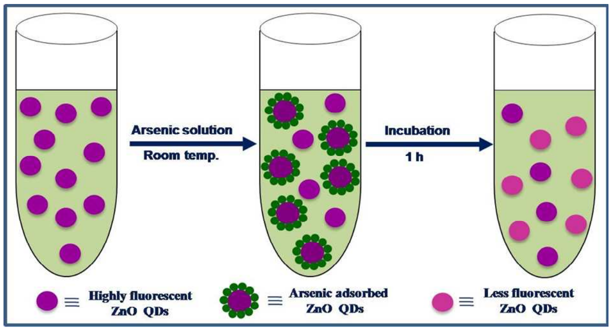

Scheme 1. Schematic presentation showing the fluorescence quenching of ZnO quantum dots in the presence of arsenic analytes

To ensure the validity of this fluorimetric method in real sample analysis, the proposed method has been applied for total arsenic determination in the underground water samples of three different places of Barak Valley, Assam, India. The real water samples were treated with 10 mM EDTA^{4-} for complexation with other metal cations but could not form complexes with arsenite/arsenate as these exists in the anionic forms. The pH of all the solutions was adjusted to ~7.0 with sodium phosphate buffer solution. Comparative analysis of three different samples by atomic absorption spectrometry and the present method (an average of three determinations) is summarised in Table 2. Similar results with atomic absorption spectrometry demonstrate the sensitivity of the proposed method for the fluorimetric determination in arsenic in real groundwater samples. A comparative account of different electrochemical and spectroscopic techniques developed for arsenic determination in aqueous solution is enunciated in Table 3. In addition, Burakham group[46] have reported a hybrid sequential injection–stopped flow injection system for the speciation of arsenic based on the quenching of mercaptoacetic acid capped cadmium sulfide quantum dots fluorescence intensity. The analytical procedure involves the generation of arsine from As(III) by sodium borohydride in acetate buffer medium at pH~6.0 and under optimal conditions, the limits of detection were found to be 20 μg L^{-1} for As(III) and 40 μg L^{-1} for As(V). A closer inspection reveals that the present method is competitive to other spectroscopic techniques[15,22,46] in terms of sensitivity but superior in the viewpoint of simplicity that the method of determination is based on the fluorescence quenching of only ZnO QDs without any further surface modification and devoid of any other substances in the dispersion medium. In the present experiment, 'stabiliser free' particles offer more accessible surface to the foreign ions than the 'ligand-stabilised' particles and as a result, the adsorption of the metal ions to the surface of the particles becomes facile. Moreover, the surface-to-volume ratio becomes higher as the particle size decreases that governs 'ultrasmall particles' to be more reactive and therefore, could adsorb metal ions to a greater extent than the larger particles. Overall, these two factors, collectively, facilitate the adsorption of metal ions on the surface of the QDs and make it possible to determine the concentration of arsenic at the ppb level. Furthermore, since the synthesis of ZnO QDs is based on the hydrolysis of the precursor salt in an alkaline medium, the particles are easy to synthesise in the milligram scale, could be stored as powder and utilised as and whenever required that deserve their potential application in routine analysis of arsenic in aquatic environment.

4. Conclusion

In summary, we have demonstrated a green strategy utilising nanotechnology for the selective and sensitive determination of arsenic in water samples. It has been found that the

Table 3. **A comparative account of different electrochemical and spectroscopic methods developed for arsenic determination in aqueous solution**

Method	Materials	Sample	Dynamic Range (ppb)	LOD (ppb)	Reference
Anodic stripping Voltammetry	Au NPs/GC	As(III)	-	0.01	Compton et al. [16]
Flow analysis	Au NPs/GC	As(III)	15.0	0.25	Loung et al. [17]
Absorption spectroscopy	Ag/Au NPs as catalyst	As(III) & As(V)	0-110	30.0	Pal et al. [15]
Fluorescence spectroscopy	Fe_3O_4 NPs	As(III)	0-100	30.0	Liu et al. [22]
Resonance Rayleigh scattering	NP assemblies	As(III)	0.1-200	0.2	Zhou et al. [19]
Surface enhanced Raman scattering	LB assemblies of Ag NPs	As(III) & As(V)	-	1.0	Yang et al. [18]
Fluorescence spectroscopy	ZnO NPs	As(III) & As(V)	10-100	28.0	Present method

fluorescence intensity decreases linearly to the arsenic concentration and this simple dependence allows for quantitative determination of arsenic at parts-per-billion concentrations. Since fluorescence spectroscopy is the most sensitive spectroscopic technique, the proposed method is reproducible and could be easily implemented in the field detection. As the present method is based on the addition and incubation of arsenic analytes into an aquatic dispersion of fluorescent ZnO QDs, the proposed method is cost-effective, environmental friendly and not much expertise is needed. From a practical point of view, the strategy of the present method could be replicated for the determination of other hazardous substances.

Acknowledgements. We gratefully acknowledge financial support from DST, New Delhi (Project No.: SR/FT/CS-68/2010). We are thankful to Dr. Nikhil R. Jana, IACS, Kolkata for providing facilities for DLS and zeta potential measurements.

References

1. U. S. Agency for Toxic Substances and Diseases Registry (ATSDR) In *Toxicological Profile for Arsenic* 2005 http://www.atsdr.cdc.gov/toxprofiles/tp2.pdf.
2. S. C. Grund, K. Hanusch and H. U. Wolf, Arsenic and Arsenic Compounds, In *Ullmann's Encyclopedia of Industrial Chemistry,* 2005, Wiley-VCH, Weinheim.
3. P. B. Tchounwou, J. A. Centeno and A. K. Patlolla, *Mol. Cell. Biochem.*, 2004, **255**, 47–55.
4. K. R. Henke, In *Arsenic: Environmental Chemistry, Health Threats and Waste Treatment*, 2009, pp. 69–236.
5. D. van Halem, S. A. Bakker, G. L. Amy and J. C. van Dijk, *Water Eng. Sci.*, 2009, **2**, 29–34.
6. World Health Organization In *United Nations Synthesis Report on Arsenic in Drinking Water* 2001, Geneva.
7. Environmental Protection Agency 2001, Adopted 22 January 2001; Effective 23 January 2006 http://water.epa.gov/lawsregs/rulesregs/sdwa/arsenic/regulations.cfm.
8. Y. R. Ryu, S. Zhu, J. D. Budai, H. R. Chandrasekhar, P. F. Miceli and H. W. White, *J. Appl. Phys.*, 2000, **88**, 201–204.
9. M. Kidwai, In *Green Chemistry–Environmentally Benign Approaches*, InTech Europe, Croatia, 2012, Chaper 6.
10. C. Jagadish and S. eds. Pearton, In *ZnO Bulk, Thin Films, and Nanostructures* 2006, Elsevier, Oxford.
11. P. Nunes, B. Fernandes, E. Fortunato, P. Vilarinho and R. Martins, *Thin Solid Films,* 1999, **337**, 176–179.
12. Y. L. Feng, H. Y. Chen, L. C. Tian and H. Narasaki, *Anal. Chim. Acta,* 1998, **375**, 167–175.
13. K. Anezaki, I. Nakatsuka and K. Ohzenki, *Anal. Sci.,* 1999, **15**, 289–291.
14. P. Thomas and K. Sniatecki, *J. Anal. At. Spectrom*. 1995, **10**, 615–618.
15. S. Kundu, S. K. Ghosh, M. Mandal and T. Pal, *New J. Chem.,* 2002, **26**, 1081–1084.
16. X. Dai, O. Nekrassova, M. E. Hyde and R. G. Compton, *Anal. Chem.*, 2004, **76,** 5924–5929.
17. E. Majid, S. Hrapovic, Y. Liu, K. B. Male and J. H. T. Luong, *Anal. Chem.,* 2006, **78**, 762–769.
18. M. Mulvihill, A. Tao, K. Benjauthrit, J. Arnold and P. Yang, *Angew. Chem. Int. Ed.,* 2008, **47**, 6456–6460.
19. Y. Wu, S. Zhan, H. Xing, L. He, L. Xu and P. Zhou, *Nanoscale*, 2012, **4**, 6841–6849.
20. H. Cui, W. Yang, X. Li, H. Zhao and Z. Yuan, *Anal. Methods* 2012, **4**, 4176–4181.
21. R. Domínguez-González, L. González Varela and P. Bermejo-Barrera, *Talanta,* 2014, **118**, 262–269.
22. B. Liu and J. Liu, *Chem. Commun.,* 2014, **50**, 8568–8570.
23. C. Pacholski, A. Kornowski and H. Weller, *Angew. Chem. Int. Ed.* 2002, **41**, 1188–1191.
24. J. P. Wilcoxon and B. L. Abrams, *Chem. Soc. Rev.,* 2006, **35**, 1162–1194.
25. F. A. Cotton and G. Wilkinson, In *Advanced Inorganic Chemistry*, 6th ed.; 1988, Wiley-Interscience: Singapore, p 602.
26. A. P. Alivisatos, *Science,* 1996, **271**, 933–937.
27. D. C. Reynolds, D. C. Look and B. Jogai, *J. Appl. Phys.* 2001, **89**, 6189–6191.
28. F. Tuomisto, K. Saarinen, D. C. Look and G. C. Farlow, *Phys. Rev. B,* 2005, **72**, 085206–085211.
29. Z. R. Tian, J. A. Voigt, J. Liu, B. Mckenzie, M. J. Mcdermott, M. A. Rodriguez, H. Konishi and H. Xu, *Nat. Mater.,* 2003, **2**, 821–826.
30. M. Y. Ge, H. P. Wu, L. Niu, J. F. Liu, S. Y. Chen, P. Y. Shen, Y. W. Zeng, Y. W. Wang, G. Q. Zhang and J. Z. Jiang, *J. Cryst. Growth,* 2007, **305**, 162–166.
31. A. Van Dijken, E. A. Meukenkamp, D. Vanmaekelbergh and A. Meijerink, *J. Lumin.* 2000, **87**, 454–456.
32. J. C. Fan, C. C. Ling and Z. Xie, Fabrication and Characterization of As Doped p-Type ZnO Films Grown by Magnetron Sputtering, In *Optoelectronics - Materials and Techniques*, P. Predeep Eds., 2011 InTech Europe, Croatia, Ch. 16, pp. 393–420.
33. G. Kresse, O. Dulub and U. Diebold, *Phys. Rev. B*, 2003, **68**, 245409 1–15.
34. J. Lin, P. Jones, J. Guckert and E. I. Solomon, *J. Am. Chem. Soc.*, 1991, **113**, 8312–8326.
35. A. M. Liu, K. Hidajat, S. Kawi and D. Y. Zhao, *Chem. Commun.*, 2000, 1145–1146.
36. M. L. Kahn, T. Cardinal, B. Bousquet, M. Monge, V. Jubera and B. Chaudret, *Chem. Phys. Chem.,* 2006, **7**, 2392–2397.
37. M. Andres Verges, A. Mifsud and C. J. Serena, *J. Chem. Soc. Faraday Trans.,* 1990, **86**, 959–963.
38. S. Goldberg and C. T. Johnston, *J. Colloid Interface Sci.* 2001, **234**, 204–216.
39. N. Rivera-Reyna, L. Hinojosa-Reyes, J. L. Guzmán-Mar, Y. Cai, K. O'Shea and A. Hernández-Ramírez, *Photochem. Photobiol. Sci.*, 2013, **12**, 653–659.
40. J. P. Coates, *Appl. Spect. Rev.,* 1996, **31**, 179–192.
41. R. Viswanatha, H. Amenitsch and D. D.Sarma, *J. Am. Chem. Soc.,* 2007, **129**, 4470–4475.
42. P. Mulvaney, L. M. Liz-Marzan, M. Giersig and T. Ung, *J. Mater. Chem.,* 2000, **10**, 1259–1270.
43. U. Nobbmann and A. Morfesis, *Mater. Today*, 2009, **12**, 52–54.
44. T. Ito, L. Sun, M. A. Bevan and R. M. Crooks, *Langmuir*, 2004, **20***,* 6940–6945.
45. X. Zhou, X. Sun, K. L. Cooper, F. Wang, K. J. Liu and L. G. Hudson, *J. Biol. Chem.*, 2011, **286**, 22855–22863.
46. N. Butwong, S. Srijaranai, W. Ngeontae and R. Burakham, *Spectrochim. Acta A*, 2012, **97**, 17–23.

Table of Contents

Determination of arsenic in water using fluorescent ZnO quantum dots

Sudip Kumar Pal, Nargis Akhtar and Sujit Kumar Ghosh

Stabiliser-free zinc oxide quantum dots have been utilised as a greener sensing platform **for the quantification of arsenic in parts-per-billion level**. The method is free from common interferences and applicable for real sample analysis.